FULL ARTICLE

A modification for the calculation of water depth profiles in oil-treated skin by in vivo confocal Raman microscopy

Chunsik Choe[1] | Johannes Schleusener[2] | Sehyok Choe[1] | Jürgen Lademann[2] | Maxim E. Darvin[2]* ⓘ

[1]Biomedical Materials Division, Faculty of Material Science, Kim Il Sung University, Pyongyang, DPR Korea

[2]Department of Dermatology, Venerology and Allergology, Center of Experimental and Applied Cutaneous Physiology, Charité Universitätsmedizin Berlin, Berlin, Germany

*Correspondence
Maxim E. Darvin, Department of Dermatology, Venerology and Allergology, Center of Experimental and Applied Cutaneous Physiology, Charité Universitätsmedizin Berlin, Charitéplatz 1, Berlin 10117, Germany.
Email: maxim.darvin@charite.de

Abstract

In this study, an extended calculation method for the determination of the water profiles in oil-treated skin is proposed, which is based on the calculation of the ratio between the Raman band intensities of water (3350-3550 cm^{-1}) and keratin

Amide I at 1650 cm^{-1}. The proposed method is compared with the conventional method based on the ratio of the Raman band intensities of water (3350-3550 cm^{-1}) and keratin at 2930 cm^{-1}. The conventional method creates artifacts in the depth profiles of the water concentration in oil-treated skin, showing a lower amount of water in the upper and intermediate layers of the stratum corneum, which is due to the superposition of oil- and keratin-related Raman bands at 2930 cm^{-1}. The proposed extended method shows no artifacts and has the potential to determine the water depth profiles after topical application of formulations on the skin.

KEYWORDS
cosmetics, skin barrier function, skin hydration, stratum corneum, topical application
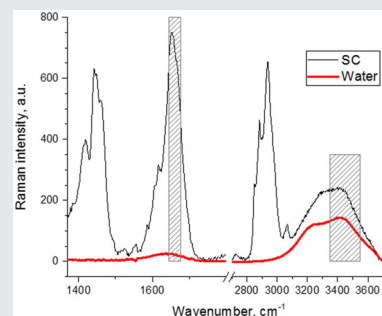
1 | INTRODUCTION

Water is an important substance for living organisms. It takes part in the cell metabolism and provides skin hydration [1]. Moreover, the water in the stratum corneum (SC) is of great importance [2, 3] in dermatology and cosmetology, regarding the proteolysis of filaggrin to natural moisturizing factor (NMF)

molecules, enzymatic activity involved in acidification, desquamation and to access the moisturizing effect [4, 5]. Water plays a critical role in maintaining the skin barrier function and to support the normal desquamation of the corneocytes [4–7]. Various analytical methodologies have been employed to measure water in the SC [8], for example, infrared spectroscopy [9–11], electrical capacitance [12], trans-epidermal water loss (TEWL) [13, 14] and confocal Raman microscopy (CRM) [12, 15, 16]. Among them, Raman spectroscopy is considered a powerful method to accurately measure water mass percentage depth profiles in the SC [17–22]. Huizinga et al [23] introduced a method using the depth profiles of CRM of the eye and calculated water profiles in the high wavenumber region (HWN) by the ratio

of the OH water band (3350-3550 cm^{-1}) to the keratin CH$_3$ band (2910-2965 cm^{-1}). Caspers et al [24] further adapted this method quantitatively for the SC in vivo [25], which evolved to be the conventional method in dermatological and cosmetic research using in vivo CRM [12, 26, 27].

However, this method cannot be successfully applied on skin treated with formulations, such as for instance, oils [28]. The 2910-2965 cm^{-1} region, which results from CH$_3$ vibrations of keratin and a minor contribution of lipid's CH$_2$ vibration [29], is strongly superimposed by formulation-related Raman bands, resulting in a miscalculation of the water profile in the SC. Thus, in case of formulation-treated skin, the water mass percentage calculated using the conventional method proposed by Caspers et al [24], shows lower values compared to untreated skin [30]. For example, oil-treated skin exhibited a lower amount of water in the uppermost SC layers than untreated skin, measured by Raman spectroscopy [12, 28, 30, 31]. This does not coincide with the findings that oils act as occlusive films on the skin resulting in an increase of water in the SC [32]. This miscalculation impairs the correct investigation on the effect of the topically applied formulations on the SC's water contents. In this study, an extended calculation method is presented, to exclude the influence of formulation-based Raman bands on the water mass percentage calculation in the SC for the example of oil-treated skin. The extended method is further compared to the conventional method proposed by Caspers et al [24] in oil-treated skin.

2 | MATERIALS AND METHODS

2.1 | In vivo application of substances

Six healthy volunteers (three females, three males) aged from 23 to 62 years (average 37 years) took part in this study. These volunteers were instructed not to utilize any skin care products on the forearms at least 72 hours and not to bath at least 4 hours before the beginning of the experiments. After an acclimation time of 20 minutes, two skin areas of 2×2 cm^2 size were marked on the volar forearms using a rubber barrier. The four oils, paraffin oil (Marcol 82tm; Esso SAF, Rueil-Malmaison, France), petrolatum oil (Fagron GmbH & Co.KG, Barsbüttel, Germany), jojoba oil (cold-pressed; Henry Lamotte, Bremen, Germany, free fatty acid value = 0.20) and almond oil (Afruse SL, Tarragona, Spain, free fatty acid value = 0.28) were applied to the marked skin areas at 2 mg/cm^2 and rubbed homogenously with soft rubber gloves. After 60 minutes, the remaining oil was wiped off using filter paper and CRM measurements were carried out on the treated and untreated skin areas. Approval for the measurements have been obtained from the Ethics Committee of the Charité Universitätsmedizin Berlin and all procedures complied with the Declaration of Helsinki.

2.2 | Confocal Raman microscopy

Raman spectra were obtained by using the CRM Model 3510 for in vivo skin measurements (River Diagnostics, Rotterdam, Netherlands). Two different lasers were used to analyze the skin in the fingerprint (FP, 400-2000 cm^{-1}) region with the excitation wavelength 785 nm and in the HWN (2000-4000 cm^{-1}) region with the excitation wavelength of 671 nm. The spatial and spectral resolutions were 5 μm and 2 cm^{-1}, respectively. Raman spectra were recorded from the skin surface down to the depth of 40 μm with 2 μm increments. The exposure time for one spectrum was 5 seconds in the FP region and 1 second in the HWN region. For each measuring position, the spectra of both regions were sequentially obtained. In detail, the recording of spectra in the FP region started at a position above the skin surface ($\approx$6-10 μm), which is denoted as mechanical starting point (MSP) and the microscope objective moved approximately 40 μm towards the skin in 2 μm increments. Then, in order to measure the HWN spectra, the microscope objective returned to this MSP, and the spectra in the HWN region were recorded accordingly. The MSP, where the microscope objective started to measure the profiles for both HWN and FP, is the criterion to compare the depth profiles of the FP and HWN measurements. The utilized CRM system was described in detail elsewhere [15, 24, 33].

2.2.1 | The calculation of the mass percentage of water in the SC

In this work, two methods were applied to calculate the water mass percentage in the SC. In the conventional method, the water mass percentage was calculated in the HWN region, by calculating the ratio of the area under the curve (AUC) of the OH Raman band (3350-3550 cm^{-1}) to the CH$_3$ vibration band of keratin (2910-2965 cm^{-1}). Here, a linear baseline was applied on the 2720 to 3790 cm^{-1} region to remove the fluorescence background. Then, the water content was calculated using Equation (1) as described elsewhere [24]:

$$\text{water content} (\%) = \frac{W_{\text{HWN}}/P_{\text{HWN}}}{W_{\text{HWN}}/P_{\text{HWN}} + R} \tag{1}$$

Here, W_{HWN} is the AUC of the water band (3350-3550 cm^{-1}), P_{HWN} is the AUC of the protein band (2910-2965 cm^{-1}) and R is a constant that was determined as 2 through the calibration process [24].

In the extended method, the water mass percentage was calculated by using the ratio of the AUCs of the OH Raman band of water (3350-3550 cm^{-1}) to the Amide I band of keratin ($\approx$1650 cm^{-1}), P_{FP}.

2.2.2 | The consideration of water contribution in the Amide I peak (1650 cm^{-1})

The drawback in applying the extended method for the water calculation in the SC is that the Amide I peak (1650 cm^{-1}) has a contribution of water around 1640 cm^{-1} (Figure 1).

As shown in Figure 1, the Raman peak intensity of the Amide I band at $\approx$1650 cm^{-1} (AUC$_{1650}$), measured as an AUC in the 1644 to 1676 cm^{-1} region, contains mostly a contribution of proteins (P_{FP}) and a small amount of water (W_{FP}), whose broad Raman peak is centered at around 1640 cm^{-1}. Thus, AUC$_{1650}$ = P_{FP} + W_{FP}. In order to estimate the contribution of water to the Amide I band of the SC, the Raman spectra of distilled water have been measured. Subsequently, the ratio of the water-related Raman peak intensities, that is, the AUCs of 1644 to 1676 cm^{-1} (W_{FP}) and 3350 to 3550 cm^{-1} (W_{HWN}), was calculated, and denoted as R_W = W_{FP}/W_{HWN}, which was experimentally determined as 0.014 $\pm$ 0.002 for distilled water. After calculating the R_W ratio for distilled water, it was applied for skin analysis to calculate the water contribution to the Amide I band as shown in Equation (2):

$$\text{water content} = \frac{W_{HWN}}{P_{FP}} = \frac{W_{HWN}}{\text{AUC}_{1650} - R_W W_{HWN}}. \quad (2)$$

It should be taken into consideration that the application of the proposed extended method requires a time-stable output power of both lasers for the excitation in the FP and HWN regions, which should be additionally proven during the measurements.
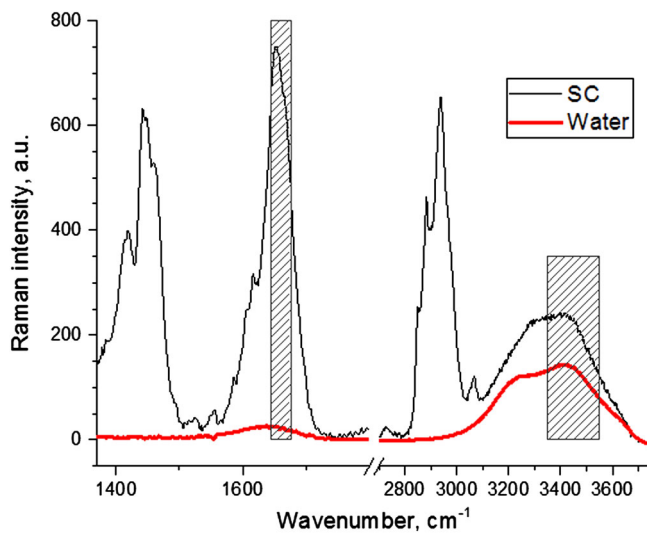
FIGURE 1 Raman spectra of untreated skin in vivo at 7.5 μm depth (black line) and pure distilled water (thick red line). The shaded rectangles represent the integration range for the Amide I band in the 1644 to 1676 cm^{-1} region and the OH vibration band in the 3350 to 3550 cm^{-1} region

2.2.3 | Calibration of the water mass percentage

The W_{HWN}/P_{FP} ratio in Equation (2) represents the relative amount of water, as opposed to the absolute value presented in Equation (1). In order to assimilate the water mass percentage in the skin to that calculated in Equation (1), the following calibration process was applied.

Firstly, for untreated skin, the values of water concentration were calculated for the same samples by Equation (1) (conventional method) and Equation (2) (extended method) using the same linear baseline subtraction in the range of 2720 to 3790 cm^{-1}. Secondly, by reversely solving Equation (1), the W_{HWN}/P_{HWN} ratios were calculated. Thirdly, linear least squares regression was applied for the W_{HWN}/P_{HWN} and W_{HWN}/P_{FP} ratios. By calculating the relationship between W_{HWN}/P_{HWN} and W_{HWN}/P_{FP}, Equation (1) was reconstructed based on Equation (2):

$$\text{water content}\,(\%) = \frac{a \times \frac{w}{P_{FP}} + b}{\left(a \times \frac{W_{HWN}}{P_{FP}} + b\right) + R} \quad (3)$$

Here, the coefficients a and b are obtained from the least squares regression between W_{HWN}/P_{HWN} and W_{HWN}/P_{FP} and their values are approximately 0.35 and 0.6, respectively (R^2 = 0.9). The obtained high correlation additionally confirm that Raman peaks at $\approx$1650 and $\approx$2935 cm^{-1} are related to one substance, that is, keratin, and the influence of other substances, for instance water and specific NMF molecules on the peak at $\approx$1650 cm^{-1} is negligible.

2.2.4 | The AUC of the Amide I band in almond oil- and jojoba oil-treated skin

As shown in Figure 2, paraffin and petrolatum oils have no Raman peaks around 1650 cm^{-1}. Therefore, the extended method is easier applicable for paraffin- and petrolatum-treated skin. Meanwhile, the conventional method might give incorrect results, because of the overlapping spectra of oils on skin in the 2910 to 2965 cm^{-1} protein-related region. Thus, the application of the extended method on paraffin and petrolatum-treated skin is more feasible than the conventional method. In the case of almond oil- and jojoba oil-treated skin, there is an oil contribution on the peak around 1650 cm^{-1}. Therefore, the extended method is also not directly applicable and the contribution of almond- and jojoba oils' Raman spectra on the Amide I band should be removed. Unlike the FP spectra of paraffin, petrolatum, almond and jojoba oils have a peak at 1740 cm^{-1}, which is not present in the SC. This peak is associated to C═O vibrations of esters [34–36], as the vegetable oils are a mixture of triglycerides and free fatty acids.
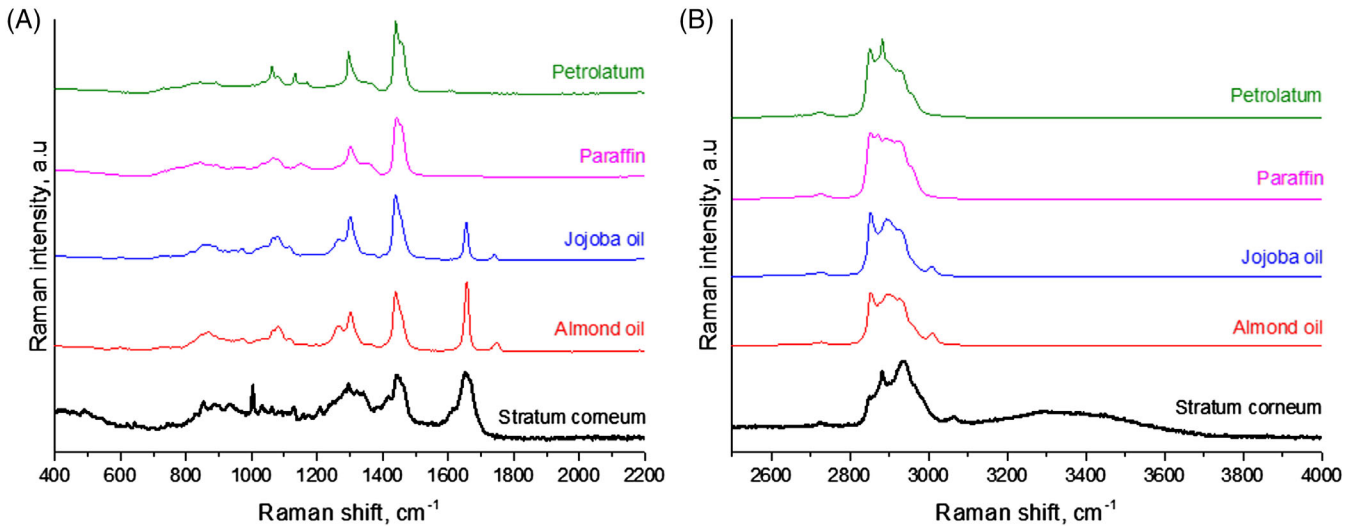
FIGURE 2 Raman spectra of almond oil (red line), jojoba oil (blue line), paraffin (magenta line), petrolatum (green line) and in vivo human stratum corneum in 4 μm depth (thick black line) in the fingerprint (A) and high wavenumber (B) regions [30]. For visibility, Raman intensities of human skin are multiplied by 4.5 and spectra are shown offset

The extended method to calculate the AUC of the Amide I band in almond- and jojoba oil-treated skin spectra by using the AUC of the peak at 1740 cm^{-1} consists of multiple steps. Firstly, the AUC ratios between the Amide I band and the Raman peak at 1740 cm^{-1} in pure almond and jojoba oils' spectra were calculated, respectively ($R_{almond} = 8.8 \pm 0.06$; $R_{jojoba} = 8.5 \pm 0.06$). Then, by using the AUC of the 1740 cm^{-1} peak and the R_{almond} and R_{jojoba} values, the contribution of oils to the Amide I band was successively removed in the spectra of oil-treated skin.

In calculating the contribution of the oils to the Amide I bands, the precise calculation of the AUC of the 1740 cm^{-1} band is important. As the peak at 1740 cm^{-1} is adjacent to the Amide I band, a baseline removal in the 1660-2200 cm^{-1} range is carried out by non-linear regression of a Lorentz function to model the baseline of fluorescence and the Amide I band for the 1740 cm^{-1} peak by selecting the points between 1688 and 1824 cm^{-1}. Furthermore, the curves around 1684 to 1830 cm^{-1} in untreated skin correspond to the part of a Lorentz function [37, 38].

The calculation of the water mass percentage in almond- and jojoba oil-treated skin is performed as follows: (a) the SC depth profiles of the AUC of the 1740 cm^{-1} peak are calculated, (b) the contribution of oils at 1740 cm^{-1} to the Amide I band is removed from the AUC of the peak at 1650 cm^{-1}, (c) by using these depth profiles of the Amide I band, the surface point is determined, (d) the W_{HWN}/P_{FP} value is calculated according to Equation (2) and finally, the water mass percentage is calculated according to Equation (3).

For petrolatum- and paraffin- oil-treated skin, the procedure is as follows: (a) by using the depth profiles of the AUC of the Amide I band, the surface point is determined, (b) the W_{HWN}/P_{FP} value is calculated according to Equation (2) and finally the water mass percentage is calculated according to Equation (3).

2.2.5 | Calculation of the skin surface

For the conventional method, the surface of the skin was determined by using the AUC depth profile of the keratin peak in the HWN region (2910-2965 cm^{-1}), as proposed by Caspers et al [24], while for the extended method, the AUC depth profile of the 1650 cm^{-1} keratin peak was used. The skin surface (0 μm) was determined to be at the position where the keratin profiles reached the half of their maxima obtained from the keratin (HWN) [24] and Amide I band, which were shown to be identical [39] in untreated skin.

2.2.6 | Normalization of the SC depth

The water depth profiles of each volunteer were averaged and the outliers were deleted from the calculations. Thereafter, the depth profiles normalized by the SC thickness to 100% and interpolated to 10% increments were averaged for six volunteers.

3 | RESULTS AND DISCUSSION

3.1 | The water profiles obtained by the conventional and extended methods

Both methods can be employed for the calculation of the amount of water in untreated SC. However, in oil-treated

skin, the superposition of the oil-related Raman bands on the keratin region (2910-2965 cm^{-1}), disturb the correct calculation of the water mass percentage (Figure 2). This effect is most prominent in petrolatum-treated skin [28], where petrolatum has a larger Raman scattering cross section compared to the other oils [31]. A similar superposition in the HWN region is expected for most cosmetic and medical formulations [34]. Therefore, it is important to calculate the water mass percentage correctly by considering the Raman spectra of oils and skin.

The water mass percentage profiles of untreated- and oil-treated skin calculated by the conventional and extended methods are presented in Figure 3. As shown in Figure 3, there are only slight differences between the water depth profiles calculated by both methods in untreated skin, while the differences are very prominent in oil-treated skin, especially in the uppermost layers of the SC.

3.2 | Comparison of the amount of water in oil-treated skin

Figure 3 shows that the water mass percentage increases towards the bottom of the SC and reaches a plateau at the boundary between the SC and the stratum granulosum, for oil-treated and untreated skin, regardless of the applied calculation method. Comparing the water profiles obtained using both methods, two differences are obvious.

1. In the uppermost layers of the SC (0%-20% SC depth), the calculation using the conventional method shows a significantly higher water mass percentage in untreated skin than in oil-treated skin (38% vs 29%, on average, Figure 3A,C). This does not coincide with previous studies. By using confocal laser scanning microscopy, Patzelt et al [40] showed that topically applied petrolatum acts as a protective film, causing a decrease of TEWL. Therefore,
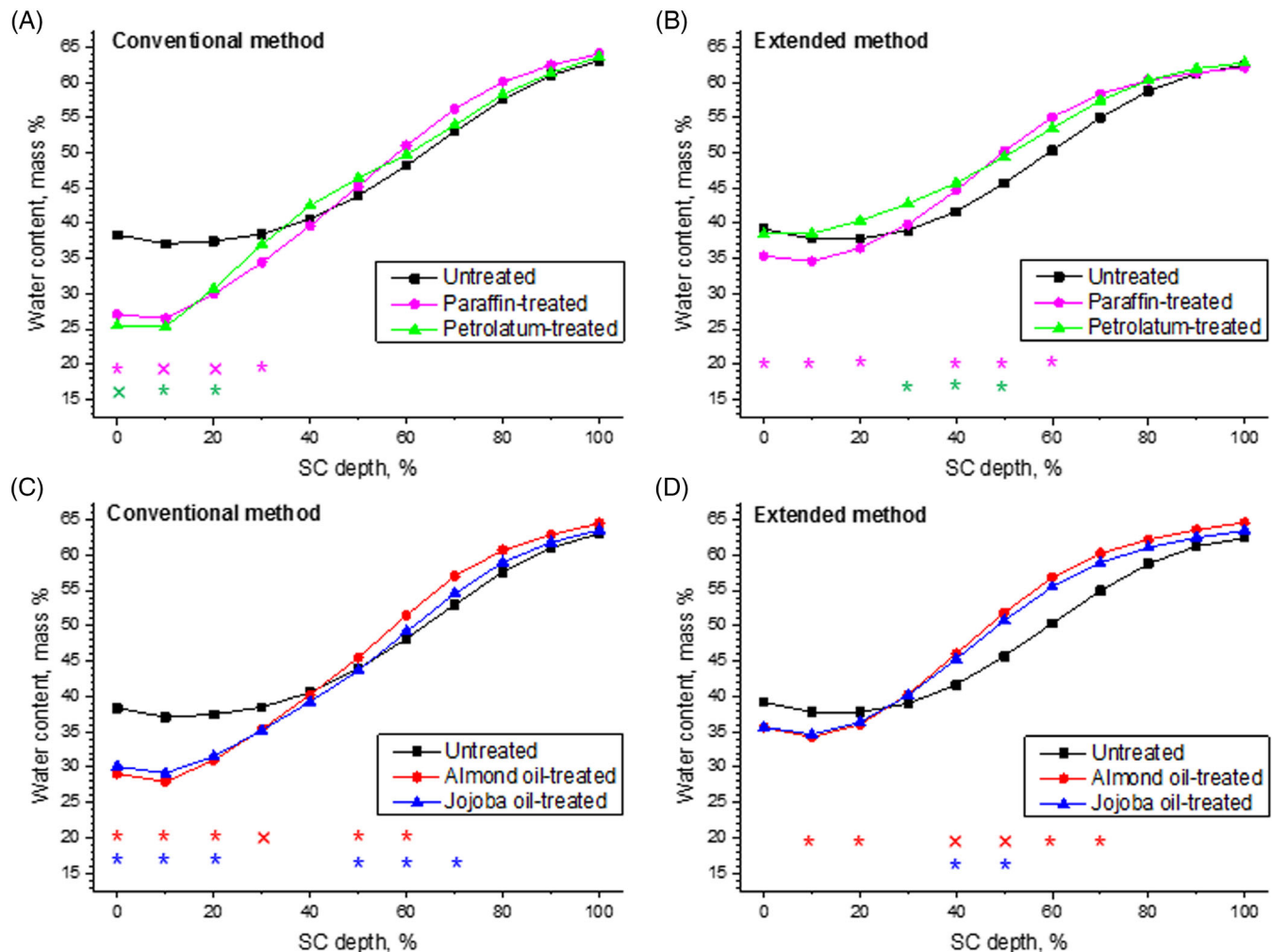
FIGURE 3 Depth profiles of water mass percentage in the stratum corneum determined by the conventional (A, C) and extended (B, D) methods. Paraffin-treated (magenta line, A, B), petrolatum-treated (green line, A, B), almond oil-treated (red line, C, D) and jojoba oil-treated (blue line, C, D) skin is determined using both methods. "*" represents significant ($P < .05$) and "×" highly significant ($P < .01$) differences to the untreated skin

it has been postulated, that the oils create occlusive films on the skin surface and thus, at the upper layers of the SC, a significantly lower amount of water in petrolatum-treated skin, that is, a drier SC compared to untreated skin is hardly explainable. Meanwhile, Figure 3B shows no significant difference of water mass percentage between untreated- and petrolatum-treated skin in the uppermost SC layers (38% vs 39%, on average) calculated using the extended method. For skin treated with the other oils, the difference to untreated skin of the water mass percentage in the upper SC layers are smaller for the extended method (38% vs 37%, on average, Figure 3B,D) than for the conventional method (38% vs 29%, on average, Figure 3A,C). Actually, the water mass percentage in the oil-treated uppermost layers of the SC (0%-20% SC depth) calculated by the extended method is higher than if calculated by the conventional method (36% vs 29%, on average for all oils, Figure 3A-D), which shows that the exceptionally lower water mass percentage in oil-treated skin determined by the conventional method might be artifactual in the upper layers of the SC, where the oils penetrate [41]. The insignificantly lower water mass percentage in the upper SC layers calculated by the extended method (~2%, Figure 3B,D) is explained by the presence of oils in these SC depths [30].

2. In the intermediate layers of the SC (30%-70% SC depth), the water profiles presented in Figure 3B,D are prominently different to the ones presented in Figure 3A,C. Figure 3B shows a larger water mass percentage in mineral oil-treated skin compared to untreated skin ($P < .05$ for petrolatum-treated skin at 30%-50% SC depth and for the paraffin-treated skin at 40%-60% SC depth). Meanwhile, using the conventional method (Figure 3A), no difference of water mass percentage between petrolatum- and paraffin-treated and untreated skin in the intermediate SC layers were obtained. For vegetable oil-treated skin, similar tendencies appear (Figure 3C,D). Although there are small differences in water mass percentage in jojoba oil-treated skin at 50% to 70% SC depths ($P < .05$) calculated by the conventional method (Figure 3C), these differences are larger by using the extended method. The differences of the average water mass percentage between jojoba and almond oil-treated and untreated skin are <2% of the water mass percentage at 60% to 70% SC depths determined by the conventional method (Figure 3A,C). However, the application of the extended method (Figure 3B,D) shows a larger amount of water mass percentage in jojoba and almond oil-treated skin, that is, ≈5% water mass percentage compared to untreated skin at 40% to 60% of the SC depth. The average water mass percentage in the 30% to 70% SC depth is similar for untreated- and oil-treated skin (~45%), calculated using the conventional method, but is increased (45% vs 50%) using extended method.

Summarizing the results of Figure 3, the conventional method is not suitable for calculating the water concentration in oil-treated skin due to following reasons. At the upper layers of the SC, the conventional method shows an exceptionally lower amount of water in oil-treated skin, which is an artifact and can be explained by overlapping of oil-derived Raman bands on the skin-related Raman bands in the 2910 to 2965 cm^{-1} region [28]. Secondly, in the intermediate layers of the SC (40%-60% SC depths), Figure 3A does not show any differences between oil-treated and untreated skin. This is in contradiction to results of previous studies that the SC can be categorized into three layers according to the SC swelling and water bonding properties, that is, the upper and bottom regions of the SC are non-swelling and furthermore, the intermediate regions determine the highest swelling [42, 43]. By using cryo scanning electron microscopy, Caussin et al [43] revealed, that petrolatum-treated SC swells mostly at the intermediate layers, indicating a larger amount of water in these layers. These findings coincide with the results presented in Figure 3B,D obtained using the extended method, which showed an increase of water mass percentage at the intermediate layers (thus, the apparent swelling of corneocytes) and no differences of water mass percentage in the upper and bottom regions of the SC (non-swelled SC regions) [42].

The differences between Figure 3A-D could be explained as follows. Firstly, the artifacts of the lower amount of water at the uppermost layers (Figure 3A,C), are caused by the overlapping of oil-derived Raman bands on the keratin band in the HWN region (see Figure 2). At the intermediate layers, the differences between both methods cannot be explained by the oils' Raman spectra, because the oils do not penetrate into the intermediate SC regions [28, 30]. In order to explain these differences in water mass percentage of the intermediate SC regions between the two methods, the surface point-settings determined using the conventional and extended methods were considered, which is shown in Figure 4.

Figure 4 shows the distances from the MSP to the surface point in petrolatum-treated skin (Figure 4A) and the distances from the MSP to the maximum point of the keratin profiles in petrolatum-treated skin (Figure 4B). The keratin profiles were obtained in the HWN (2930 cm^{-1}, conventional method) and FP (1650 cm^{-1}, extended method) regions, respectively. Figure 4A clearly shows the differences in setting the surface points in the HWN and the FP regions in petrolatum-treated skin. The values obtained in the HWN region are 2.3 ± 1.1 μm smaller than those obtained in the FP region.

Meanwhile, it was already reported that in untreated skin, there are no differences in the distances from the MSP to the skin surface, regardless if the keratin profiles were calculated in the HWN or FP region [39]. That is, the surface points determined by the Amide I band in the FP region and the
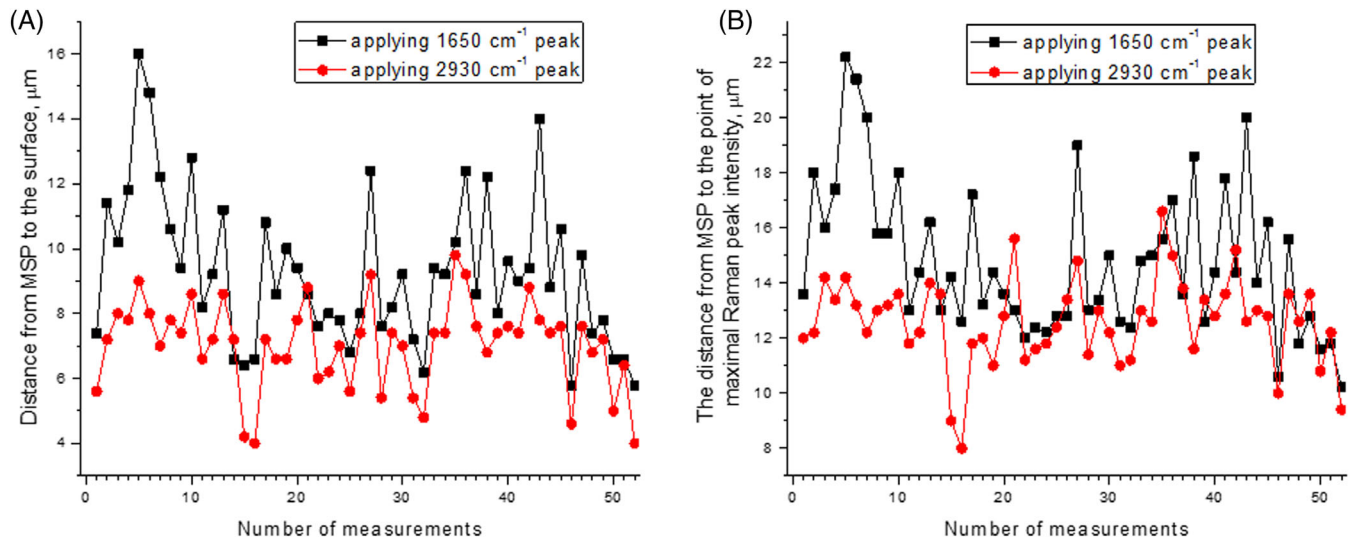
FIGURE 4 The distance from mechanical starting point (MSP) to the surface point (A) and the distance from MSP to the position of maximal keratin intensity (B) for 52 measuring points on six volunteers in petrolatum-treated skin. Red circles represent the measuring points of the keratin profile calculated from the high wavenumber region (2910-2965 cm^{-1}, conventional method) and the black rectangles represent data points determined from the keratin profiles that were obtained from the Amide I band in the fingerprint region (1642-1676 cm^{-1}, extended method)

ones determined by keratin in the HWN region coincide in untreated skin. The differences in untreated skin are about -0.1 ± 0.4 µm ($P > .05$). Therefore, we conclude that the obtained differences in petrolatum-treated skin (Figure 4A) are caused by the keratin peak in the HWN region (2935 cm^{-1}), which was already superimposed by the oils' Raman band (Figure 2). As shown in Figure 4B, there is also a difference in the distance from the MSP to the maximum of the keratin profiles obtained from the HWN and FP regions, respectively. It was also reported, that in untreated skin, no differences in the maximum points were found [39]. The distances from the MSP to the maximum point in petrolatum-treated skin is by 2.2 ± 1.6 µm smaller in the HWN than in the FP region. This shift of the maximum points towards the surface of the skin in the HWN region can be explained as follows (Figure 5): The keratin peak around 2935 cm^{-1}, which is the sum of the keratin spectra of skin and the oil-derived CH_3 vibration band, will be increased at the upper layers, since most oils are highly concentrated in the superficial layers of the SC [30]. This causes the shift of the maximum points towards the surface position (Figure 4). Since the surface point is determined by the half maximum of the depth profiles of keratin (Figure 4), it is also shifted towards the surface of the skin by moving the maximum points towards the surface, which is schematically presented in Figure 5. However, the Amide I band used in the extended method is not superimposed by the oil-related Raman bands (Figure 2) or the oil's contribution is removed. Therefore, the shift of the surface points does not occur, indicating the correct position of the skin surface points. The effect of a shifting surface point in the treated skin should be taken
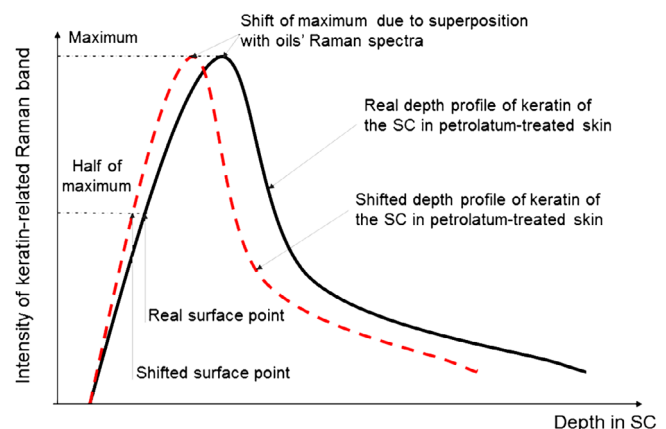
FIGURE 5 The scheme of shifting of the keratin profile by the presence of oils in the upper stratum corneum layers

into consideration by analyzing the penetration profiles of xenobiotics into the SC [27, 44–47], where the determination of the correct surface position is very important.

Consequently, the mismatch occurs between the surface points determined by the Amide I band in the FP region (extended method) and by keratin in the HWN region (conventional method). This miscalculation in setting the surface points causes a miscalculation of the overall depth profile of water by using the conventional method. It is suspected that by shifting the water depth profile of oil-treated skin (Figure 3A,C), 2 to 3 µm towards the skin surface, an increase of water will likely appear and might be present in the profiles in Figure 3B,C. However, even in this case, the lower amount of water at the upper layers of the SC will not be recovered, which indicates that the Amide I band (extended method)

should be used to correctly calculate the water mass percentage throughout the entire SC.

4 | CONCLUSION

In this study, an extended method was developed to calculate the water mass percentage in the SC of untreated and oil-treated skin, and was compared to the conventional method. The conventional method based on the calculation of the ratio of water (HWN: 3350-3550 cm^{-1}) to keratin (HWN: 2910-2965 cm^{-1}), is applicable in untreated skin, but creates artifacts in oil-treated skin due to overlapping of Raman peaks in the HWN region (2910-2965 cm^{-1}). Particularly in the upper and intermediate layers of the SC, the conventional method might not be applicable on calculating water profiles in oil-treated skin and does not correlate with the results obtained by using other methods, such as confocal laser scanning microcopy and cryo scanning electron microscopy. This might not only occur in oil-treated skin, but also in skin-treated with cosmetics or medical ointments that have an inherent Raman contribution in the 2910 to 2965 cm^{-1} region. Therefore, previous results obtained using the conventional method might have to be reconsidered in drug-treated skin, taking the influence of substance-related Raman bands on the keratin band in the HWN region into account. For example, the surface points can be artifactually shifted by the substance-related bands. In this respect, the proposed extended method, that uses the Amide I band in the FP region, is appropriate for the calculation of the water concentration in oil-treated skin. If the applied substances expose a Raman contribution in the region of the Amide I band-like almond and jojoba oils, the contribution of these peaks should be reasonably considered. The recalculated water profiles also confirmed that the intermediate layers of the SC have a propensity to swell by topical applied moisturizers, compared with the upper and bottom layers of the SC and there is no decrease of water in the upper layers of the SC, which was not shown until now in Raman studies of the oils-treated skin. The proposed extended method has a high potential in investigating the moisturizing effect of topically applied cosmetic and medical formulations on the SC without showing artifacts.

CONFLICT OF INTEREST

The authors declare no financial or commercial conflict of interest.

AUTHOR CONTRIBUTIONS

M.E.D., J.L. and C.S.C. conceptualized the experiments and designed the research. C.S.C. and M.E.D. performed the research. S.H.C. and J.S. performed data analysis and interpretation. All authors have contributed to the development of the methodology and in preparation of the manuscript.

DATA AVAILABILITY STATEMENT

The data that support the findings of this study are available from the corresponding author upon reasonable request.

ORCID

Maxim E. Darvin https://orcid.org/0000-0003-1075-1994

REFERENCES

[1] N. Watanabe, K. Suga, H. Umakoshi, *J. Chem.* **2019**, *2019*, 15.

[2] J. -L. Lévêque. Bioengineering of the Skin. (Eds: J. W. Fluhr, P. Elsner, E. Berardesca, H. I. Maibach) *Water-Keratin Interactions*. Boca Raton, FL, CRC Press; **2005**, *2*, 15.

[3] B. B. Michniak, P. W. Wertz, Bioengineering of the Skin. (Eds: J. W. Fluhr, P. Elsner, E. Berardesca, H. I. Maibach) *Water-Lipid Interactions*. Boca Raton, FL, CRC Press; **2005**, *2*, 3.

[4] A. V. Rawlings, *J. Pharm. Pharmacol.* **2010**, *62*, 671.

[5] A. V. Rawlings, P. J. Matts, *J. Invest. Dermatol.* **2005**, *124*, 1099.

[6] A. Rawlings, C. Harding, A. Watkinson, J. Banks, C. Ackerman, R. Sabin, *Arch. Dermatol. Res.* **1995**, *287*, 457.

[7] P. M. Elias, K. R. Feingold, Skin Barrier. (Eds: P. M. Elias, K. R. Feingold) *Stratum Corneum Barrier Function: Definitions and Broad Concepts*. Boca Raton, FL, CRC Press; **2006**, *1*, 1.

[8] M. Qassem, P. Kyriacou, *Cosmetics* **2019**, *6*, 19.

[9] M. Egawa, M. Yanai, K. Kikuchi, Y. Masuda, *Appl. Spectrosc.* **2011**, *65*, 924.

[10] M. Egawa, M. Yanai, N. Maruyama, Y. Fukaya, T. Hirao, *Appl. Spectrosc.* **2015**, *69*, 481.

[11] A. Ezerskaia, N. E. Uzunbajakava, G. J. Puppels, J. de Sterke, P. J. Caspers, H. P. Urbach, B. Varghese, *Biomed. Opt. Express* **2018**, *9*, 2436.

[12] J. M. Crowther, A. Sieg, P. Blenkiron, C. Marcott, P. J. Matts, J. R. Kaczvinsky, A. V. Rawlings, *Br. J. Dermatol.* **2008**, *159*, 567.

[13] I. H. Blank, J. Moloney 3rd. , A. G. Emslie, I. Simon, C. Apt, *J. Invest. Dermatol.* **1984**, *82*, 188.

[14] N. Sekkat, Y. N. Kalia, R. H. Guy, *J. Pharm. Sci.* **2002**, *91*, 2376.

[15] P. J. Caspers, G. W. Lucassen, H. A. Bruining, G. J. Puppels, *J. Raman Spectrosc.* **2000**, *31*, 813.

[16] C. Choe, J. Lademann, M. E. Darvin, *Analyst* **2016**, *141*, 6329.

[17] M. Gniadecka, O. Faurskov Nielsen, D. H. Christensen, H. C. Wulf, *J. Invest. Dermatol.* **1998**, *110*, 393.

[18] P. D. Pudney, E. Y. Bonnist, P. J. Caspers, J. P. Gorce, C. Marriot, G. J. Puppels, S. Singleton, M. J. van der Wolf, *Appl. Spectrosc.* **2012**, *66*, 882.

[19] L. Zhang, T. Cambron, Y. Niu, Z. Xu, N. Su, H. Zheng, K. Wei, P. Ray, *Anal. Chem.* **2019**, *91*, 2784.

[20] C. Choe, J. Schleusener, J. Lademann, M. E. Darvin, *J. Biophotonics* **2018**, *11*, e201700355.

[21] A. Y. Sdobnov, M. E. Darvin, J. Schleusener, J. Lademann, V. V. Tuchin, *J. Biophotonics* **2018**, *12*, e201800283.

[22] L. E. Masson, C. M. O'Brien, I. J. Pence, J. L. Herington, J. Reese, T. G. van Leeuwen, A. Mahadevan-Jansen, *Analyst* **2018**, *143*, 6049.

[23] A. Huizinga, A. C. Bot, F. F. de Mul, G. F. Vrensen, J. Greve, *Exp. Eye Res.* **1989**, *48*, 487.

[24] P. J. Caspers, G. W. Lucassen, E. A. Carter, H. A. Bruining, G. J. Puppels, *J. Invest. Dermatol.* **2001**, *116*, 434.

[25] S. Leikin, V. A. Parsegian, W. Yang, G. E. Walrafen, *Proc. Natl. Acad. Sci. U. S. A.* **1997**, *94*, 11312.

[26] M. D. van Logtestijn, E. Dominguez-Huttinger, G. N. Stamatas, R. J. Tanaka, *PLoS One* **2015**, *10*, e0117292.

[27] V. K. Tippavajhala, T. D. Magrini, D. C. Matsuo, M. G. P. Silva, P. P. Favero, L. R. De Paula, A. A. Martin, *AAPS PharmSciTech* **2018**, *19*, 3177.

[28] C. Choe, J. Lademann, M. E. Darvin, *J. Dermatol. Sci.* **2015**, *79*, 176.

[29] C. Choe, J. Lademann, M. E. Darvin, *Analyst* **2016**, *141*, 1981.

[30] C. Choe, J. Lademann, M. E. Darvin, *Skin Pharmacol. Physiol.* **2015**, *28*, 318.

[31] G. N. Stamatas, J. de Sterke, M. Hauser, O. von Stetten, A. van der Pol, *J. Dermatol. Sci.* **2008**, *50*, 135.

[32] R. Filho, *Int. J. Cosmet. Sci.* **1997**, *19*, 65.

[33] Y. Zhu, C. S. Choe, S. Ahlberg, M. C. Meinke, U. Alexiev, J. Lademann, M. E. Darvin, *J. Biomed. Opt.* **2015**, *20*, 051006.

[34] M. de Veij, P. Vandenabeele, T. De Beer, J. P. Remon, L. Moens, *J. Raman Spectrosc.* **2009**, *40*, 297.

[35] P. Vandenabeele, B. Wehling, L. Moens, H. Edwards, M. De Reu, G. Van Hooydonk, *Anal. Chim. Acta* **2000**, *407*, 261.

[36] N. J. Kline, P. J. Treado, *J. Raman Spectrosc.* **1997**, *28*, 119.

[37] M. S. Bradley, J. H. Krech, *J. Phys. Chem.* **1993**, *97*, 575.

[38] P. Pelikán, M. Čeppan, M. Liška, *Resolution of Spectra*, CRC Press, Boca Raton, FL **1993**, p. 29.

[39] C. Choe, S. Choe, J. Schleusener, J. Lademann, M. E. Darvin, *J. Raman Spectrosc.* **2019**, *50*, 945.

[40] A. Patzelt, J. Lademann, H. Richter, M. E. Darvin, S. Schanzer, G. Thiede, W. Sterry, T. Vergou, M. Hauser, *Skin Res. Technol.* **2012**, *18*, 364.

[41] C.-S. Choe, J. Lademann, M. E. Darvin, *Laser Phys.* **2014**, *24*, 105601.

[42] C. Choe, J. Schleusener, J. Lademann, M. E. Darvin, *Sci. Rep.* **2017**, *7*, 15900.

[43] J. Caussin, H. W. Groenink, A. M. de Graaff, G. S. Gooris, J. W. Wiechers, A. C. van Aelst, J. A. Bouwstra, *Exp. Dermatol.* **2007**, *16*, 891.

[44] J. Lademann, P. J. Caspers, A. van der Pol, H. Richter, A. Patzelt, L. Zastrow, M. Darvin, W. Sterry, J. W. Fluhr, *Laser Phys. Lett.* **2009**, *6*, 76.

[45] C. Souza, P. Maia Campos, S. Schanzer, S. Albrecht, S. B. Lohan, J. Lademann, M. E. Darvin, M. C. Meinke, *Skin Pharmacol. Physiol.* **2017**, *30*, 81.

[46] L. Binder, E. M. Kulovits, R. Petz, J. Ruthofer, D. Baurecht, V. Klang, C. Valenta, *Eur. J. Pharm. Biopharm.* **2018**, *130*, 214.

[47] V. K. Tippavajhala, T. de Oliveira Mendes, A. A. Martin, *AAPS PharmSciTech* **2018**, *19*, 753.